Article

The Quantum Chemical Guided Steglich Rearrangement of Azlactones and Isoxazolones

Pedro P. de Castro, Juliana A. dos Santos, Marcelo M. de Siqueira, Gabriel M. F. Batista, Hélio F. Dos Santos, and Giovanni W. Amarante

J. Org. Chem., **Just Accepted Manuscript** • DOI: 10.1021/acs.joc.9b02099 • Publication Date (Web): 16 Sep 2019

The Quantum Chemical Guided Steglich Rearrangement of Azlactones and Isoxazolones

Pedro P. De Castro,[‡] Juliana A. Dos Santos,[‡] Marcelo M. De Siqueira, Gabriel M. F. Batista, Hélio F. Dos Santos,* and Giovanni W. Amarante*

Chemistry Department, Federal University of Juiz de Fora, Campus Martelos, Juiz de Fora, Minas Gerais 36036-900, Brazil.

* helio.santos@ufjf.edu.br

* giovanni.amarante@ufjf.edu.br

[‡] These authors contributed equally to this work.

Keywords: Steglich Rearrangement, Isoxazol-5(4H)-one, azlactone, density functional theory

ABSTRACT GRAPHIC

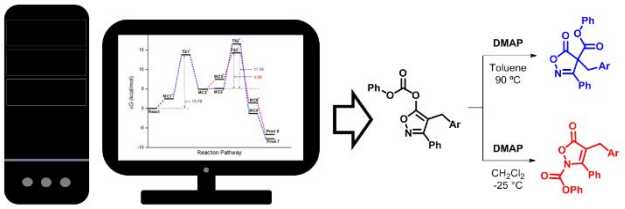

ABSTRACT

The theoretical guided evaluation of the Steglich rearrangement of azlactones and isoxazolones allowed the determination of the reactivity patterns in these heterocycles, including the factors that drive the regioselectivity towards both possible sites. These results allowed the first experimental report on the regioselective Steglich rearrangement of isoxazolones, affording the nitrogen- or carbon-acyloxy adducts.

INTRODUCTION

Organic transformations involving the formation of new carbon-carbon bonds appear as key reactions in organic synthesis, especially those that allow the formation of new stereogenic centers.[1,2] In this context, Steglich and Höfle described in 1968 the pyridine catalyzed conversion of 5-carboxyl oxazole into a 4-carboxyl azlactone derivative, a reaction that was henceforth known as the Steglich rearrangement.[3] Since its discovery, this transformation presented great development, mainly to the use of more nucleophilic organic bases (such as DMAP and 4-(pyrrolidino)pyridine), to the development of regioselective protocols for the acyloxy migration[4,5] and to the development of asymmetric protocols employing novel chiral catalysts.[6]

Concerning the azlactone substrate (also known as oxazol-5(4H)-one), several methodologies for the Steglich rearrangement have been previous described, noteworthy those

employing chiral DMAP (Schemes 1A),[7–9] co-catalytic methodologies (Scheme 1B)[10] and *N*-heterocyclic carbene organocatalysts[11] Moreover, most reports involves the acyloxy migration to the azlactone 4-position carbon, although in fewer cases the 2-position migration was also observed.[12,13]

On the other hand, to the best of our knowledge, the same transformation has not been previously described for isoxazol-5(4H)-one (Scheme 1C). Isoxazolones consist of azlactone isomers with potential application in medicinal chemistry and organic synthesis.[14–16] It is also worth mentioning that this versatile heterocycle is also present in a variety of natural products.[17]

Scheme 1. Previous reports of the Steglich rearrangement of azlactones and this study proposal

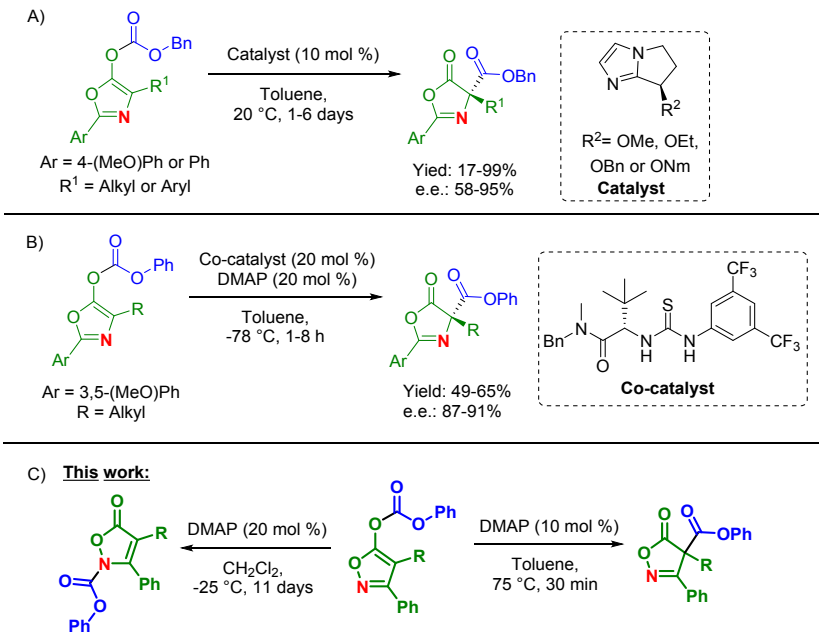

Right after its development computational methods were only employed as tools to explain empirical results after they were performed.[18] However, the rapid advent of theoretical chemistry field has made computational modeling more reliable, running into prediction of reactivities and guiding experimentalists.[19]

Recently, an interesting study involving the catalytic regiodivergent Steglich rearrangement of pyrazolyl carbonates was described by Smith's group.[20] Since, our research

group has been studying the reactivity of oxazolone rings over the last years,[21,22] we also got intrigued with azlactone reactivity in the Steglich rearrangement, that can drive the acyloxy transfer selectively to one of the reactive sites. With this purpose, we herein present a theoretical study aiming to provide new insights to explain the behavior of the azlactone ring in this process. Besides, we also present the first experimental report of the Steglich rearrangement in isoxazolones and provide a viable explanation for the divergent reactivity of these heterocycles when compared to azlactones.

COMPUTATIONAL METHODS

The calculations were performed employing the Gaussian 09 package.[23] Unless otherwise noted, all calculations were performed at a pressure equal to 1 atm and at a temperature of 298.15 K. All structures, molecular complexes (MCs) and transition states (TSs) were fully optimized in the gas phase employing the Density Functional Theory (DFT) at the M06-2X-D3/6-31G(d,p) level of theory.[24,25] Vibrational analysis was undertaken to confirm the identity of all stationary points and to allow the determination of the Gibbs free energy corrections to the reaction profile. TSs were optimized using the Berny algorithm[26] and confirmed to have only one imaginary frequency (Intrinsic Reaction Coordinates[27] were also calculated and are available in the Supporting Information).

For attainment of the electronic energy at the desired level of theory, single point energies were then subsequently calculated using the previously optimized geometries at the M06-2X-D3/6-31++G(d,p) level of theory and the Solvation Model based on Density (SMD) for toluene. The Gibbs Free Energy of each structure was then calculated by the following equation:

$$G^{\circ}_{sol} = E_{Gas} + G^{\circ}_{T} + G_{Solv}$$

In which the terms are the Electronic Energy, the thermal correction to enthalpy and entropy, and solvation Gibbs Free Energy, respectively.

RESULTS AND DISCUSSION

- **AZLACTONES**

We decided to start our investigation focusing on the azlactone scaffold, aiming to explain the regioselectivity towards the acyloxy migration. The mechanism for the Steglich rearrangement of this heterocycle is depicted in Scheme 2. Initially, an *O*-acylated azlactone (**1**) reacts with 4-(dimethylamino)pyridine, transferring the acyloxy group and thus affording an ion-pairing intermediate. The azlactone enolate formed during this step has three main resonance forms (**2a-c**), that after another acyloxy transfer can lead both to C4 (**3**) or C2 (**4**) adducts. Almost the totality of the reports in the literature describes only the formation of **3** and speculatively evokes steric and/or electronic effects to suggest this regioselectivity. Furthermore, literature data only describes azlactone acyloxy migration; thus, we also decide to evaluate if other groups, such as acyl, can also be transferred. To this purpose both acyl (R = Ph and Bn) and acyloxy (R = OPh and OBn) groups were simulated in the computational data below.

Scheme 2. Mechanism of the Steglich rearrangement of azlactones

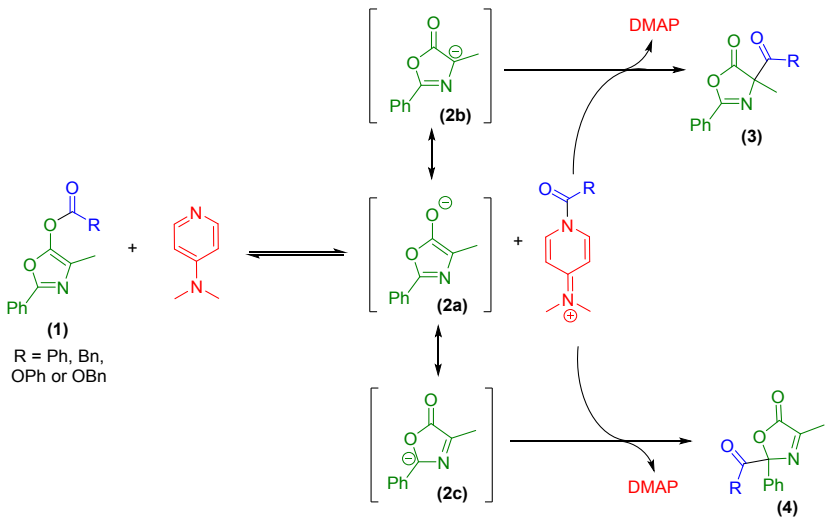

We found that the acyl/acyloxy migration of **1** to the DMAP proceeds through an elementary transition state (TS1) instead of a stepwise reaction (Figure 1) and that these TSs are very similar, independent of the substituent. For example, for R = OPh, this asynchronous TS is structurally closer to the products than to the initial reagents, presenting a C---O bond length of 1.97 Å, much longer than the C---N (1.53 Å). Furthermore, the comparison of this TS structure with the molecular complexes right before (MC1) and after (MC2) the acyloxy transfer indicates the concomitant C---N formation (bond lengths 2.71, 1.53 and 1.43 Å, respectively) and C---O bond cleavage (bond lengths 1.36, 1.97 and 2.52 Å, respectively) (the structure of all molecular complexes are available in the SI). Another important intermolecular interaction present in all these structures is the occurrence of π-stacking[28] between the azlactone heterocycle moiety and the DMAP heteroaryl group.

Figure 1. Transition states involved in the Steglich rearrangement of azlactones. The values in parenthesis corresponds to the atom distances in the molecular complexes right before and after the transition states

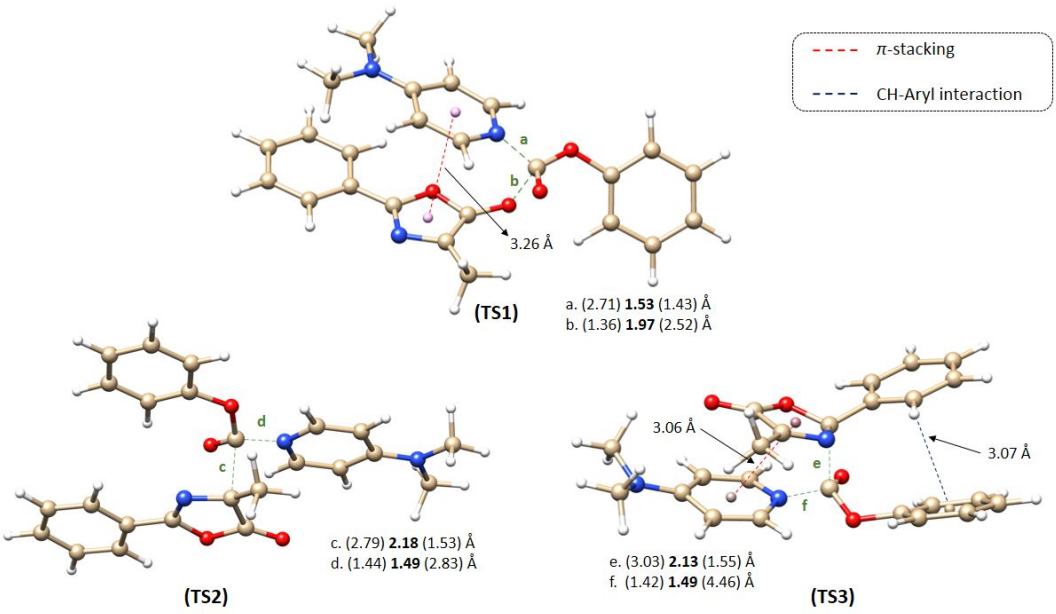

Considering the conversion of the initial species (**1** + DMAP) into the ion-pairing intermediate, it is possible to observe that during this step the barriers for the acyloxy migration is favored over acyl transfer by 2-3 kcal/mol (Table 1 – TS1), what may explain the reason for their experimental use. On the other hand, although acyl migration presents higher barriers, the barriers probably are lower enough to be accessed at room temperature/mild heating.

Table 1. Gibbs Free Energy Variation for the formation of products 3 and 4 based on the acyl/acyloxy migrating group (kcal/mol)

Substituent (R)	TS1		TS2		TS3	
	$\Delta G^{\ddagger}_{\mathbf{1\rightarrow 2a}}$	$\Delta G_{\mathbf{1\rightarrow 2a}}$	$\Delta G^{\ddagger}_{\mathbf{2b\rightarrow 3}}$	$\Delta G_{\mathbf{2b\rightarrow 3}}$	$\Delta G^{\ddagger}_{\mathbf{2c\rightarrow 4}}$	$\Delta G_{\mathbf{2c\rightarrow 4}}$
Ph	15.26	10.94	10.68	-16.58	14.93	-11.10
Bn	15.19	10.33	11.28	-16.52	15.93	-11.14
OPh	11.97	7.49	10.33	-19.49	14.30	-12.70
OBn	13.07	7.48	11.23	-19.61	15.94	-13.84

* The barriers were calculated employing the most stable species or conformers: **1**, **3** and **4** as the isolated molecules and **2a-c** as molecular complex 2 (MC2).

From this ion-pairing molecular complex (MC2), the reaction can proceed through two possible pathways, leading to **3** or **4**. Before accessing the transition states that would result in these products, two other conformers of MC2 must be accessed (hereby named MC3 and MC5). Since these molecular complexes presented higher overall energies than MC2, the barriers for these TSs were calculated employing the latter.

For the formation of **3**, the transition state (TS2) presents a C---C bond length of 2.18 Å (against 2.79 Å in MC3 and 1.53 Å in the molecular complex between product **3** and DMAP (MC4), evidencing carbon-carbon bond formation) and a N---C bond length of 1.49 Å (against 1.44 Å in MC3 and 2.83 Å in MC4, indicating bond cleavage) (Figure 1). These TSs presented barriers between 10-11 kcal/mol, independent of which substituent was employed (Table 1 – TS2). In all cases the formation of the final adducts (**3**) was greatly thermodynamically favored, with ΔG around -16 kcal/mol for the acyl derivatives and -19 kcal/mol for acyloxy adducts.

Finally, the formation of product **4** proceeds through a transition state (TS3), in which the C---C bond is being formed (bond lengths: 3.03 Å (MC5); 2.13 Å (TS3) and 1.55 Å (MC6)) simultaneously to the cleavage of the N---C bond (bond lengths: 1.42 Å (MC5); 1.49 Å (TS3) and 4.46 Å (MC6), leading to a molecular complex between **4** + DMAP (MC6). This TS presents two important intermolecular interactions: π-stacking between the azlactone enolate moiety and the DMAP pyridine group and also a noncovalent CH-Aryl interaction (Figure 1). For all substituents, the barrier for the formation of **4** is considerably higher than for accessing **3** (between 4-5 kcal/mol) and its overall reaction is less favored by 5-7 kcal/mol (Table 1 – TS3).

An overall reaction profile for the formation of both **3** and **4** is shown in Figure 2. The association of kinetics and thermodynamic drives the reaction towards product **3** and explains why almost the totality of the reports of the Steglich rearrangement of azlactones affords only the C4-product (**3**). Besides, it is also possible to observe that although the use of acyl instead of acyloxy-migrating groups might be experimentally possible, the considerably higher barrier during TS1 would probably require harsh reaction conditions.

Figure 2. Reaction pathway for the formation of products 3 and 4 (R = OPh)

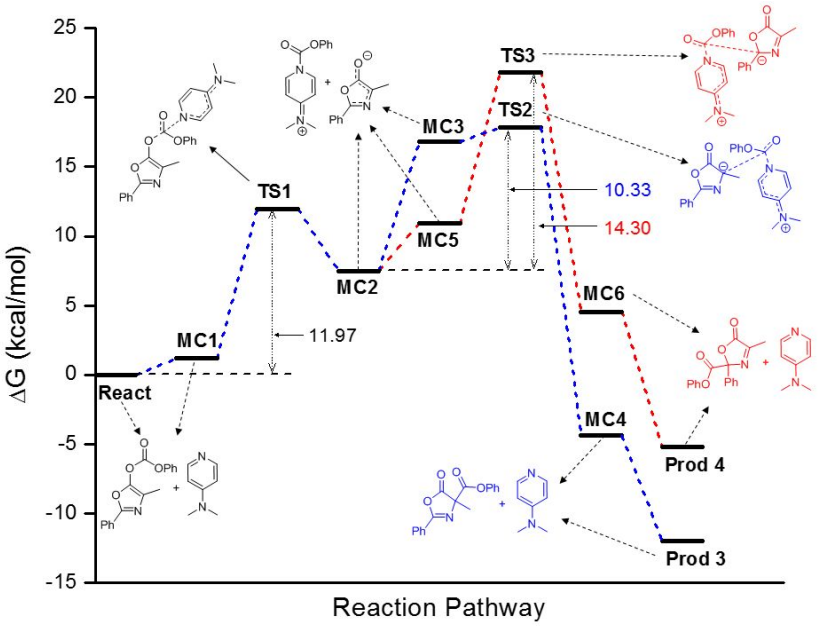

All simulations realized so far employed alanine derived azlactones, in which the heterocycle presents a 4-methyl group. Aiming to evaluate if the reaction profile can be altered by enhancing the steric hindrance at this position (and thus starting to favor product **4** over **3**), this group was substituted for ethyl, isopropyl and *tert*-butyl analogues and the overall energies are summarized in Table 2.

Table 2. Gibbs Free Energy Variation for the formation of products 3 and 4 based on the 4-azlactone substituent (kcal/mol)

C4-position Substituent[a]	TS1		TS2		TS3	
	$\Delta G^{\ddagger}_{1\rightarrow 2a}$	$\Delta G_{1\rightarrow 2a}$	$\Delta G^{\ddagger}_{2b\rightarrow 3}$	$\Delta G_{2b\rightarrow 3}$	$\Delta G^{\ddagger}_{2c\rightarrow 4}$	$\Delta G_{2c\rightarrow 4}$
Me	11.97	7.49	10.33	-19.49	14.30	-12.70
Et	12.19	7.24	9.42	-20.22	16.37	-13.75
***i*Pr**	10.41	6.84	12.14	-19.62	14.68	-13.87
***t*Bu**	13.87	10.13	16.23	-19.24	14.31	-14.63

[a] In all simulations the acyloxy migrating group was defined as OPh. * The barriers were calculated employing the most stable species or conformers: **1**, **3** and **4** as the isolated molecules and **2a-c** as molecular complex 2 (MC2).

It is possible to observe that while the reaction profile is very similar for methyl and ethyl substituents, the use of a more hindered isopropyl group promotes a slight enhancement of the TS2 barrier (2-3 kcal/mol), leading to a smaller gap between TS2/TS3 barrier and to a small regioselectivity towards product **3**. This explains why literature rarely describes the Steglich rearrangement employing valine-based azlactones.[7] On the other hand, the use of *tert*-butyl substituent completely alters the acyloxy group migration selectivity by enhancing the TS2 barrier by 4-7 kcal/mol, and thus making the formation of product **4** kinetic favored over **3**. Although in all cases the thermodynamic product remains as **3**, the use of *t*Bu is an interesting alternative for future works aiming to develop an enantioselective protocol to access **4**.

- **ISOXAZOLONES**

We next turned our attention towards the isoxazolone heterocycle. Although the Steglich rearrangement of this cycle has never been described, similarly to azlactones it can lead to two products **7** and **8** (Scheme 3). The main difference in this case is that while in **7** a carbon-carbon bond is formed, in the case of the adduct **8**, a carbamate is formed through a new carbon-nitrogen bond. Moreover, during the reaction the enolate (**6a-c**) can delocalize its charge into the more electron affinity nitrogen atom.

Scheme 3. Mechanism of the Steglich Rearrangement of isoxazolones

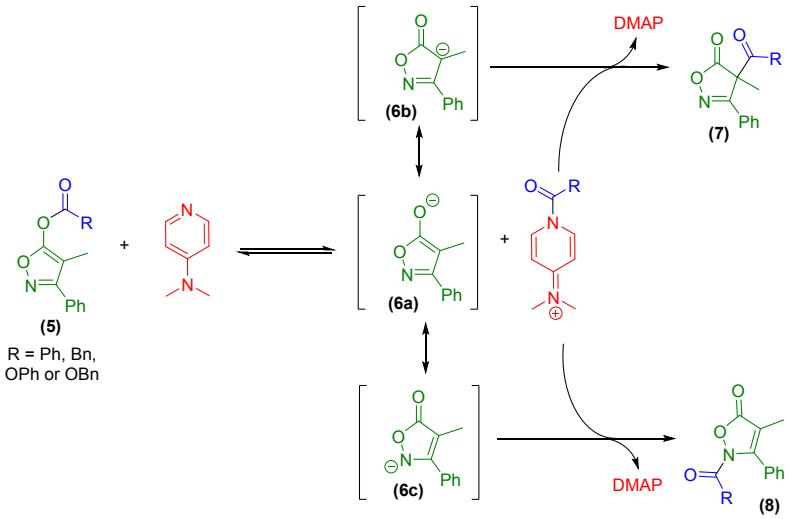

We then simulated these two pathways for the same for acyl/acyloxy migrating groups previously used for azlactones and the results are summarized in Table 3. It is possible to observe that in all cases the formation of the ion-pairing intermediate is the rate-limiting step, with barriers between 14 and 16 kcal/mol. Besides, once again the acyl migration presented slightly higher barriers for the ion pair formation (1-2 kcal/mol) than the acyloxy groups. This first transition state (hereby named TS1') is structurally related to the TS1 of azlactones, presenting π-stacking interactions between the heterocycle moiety and the DMAP pyridine ring (Figure 3). Furthermore, the comparison of bond distances in MC1', TS1' and MC2' evidences the C---O

bond cleavage (1.36 Å, 1.80 Å and 2.61 Å, respectively) and C---N bond formation (2.87 Å, 1.58 Å and 1.44 Å, respectively) (the structure of these molecular complexes are available in the SI).

Table 3. Gibbs Free Energy Variation for the formation of products 7 and 8 based on the acyl/acyloxy migrating group (kcal/mol)

Substituent (R)	TS1'		TS2'		TS3'	
	$\Delta G^{\ddagger}_{5\rightarrow 6a}$	$\Delta G_{5\rightarrow 6a}$	$\Delta G^{\ddagger}_{6b\rightarrow 7}$	$\Delta G_{6b\rightarrow 7}$	$\Delta G^{\ddagger}_{6c\rightarrow 8}$	$\Delta G_{6c\rightarrow 8}$
Ph	15.80	8.22	14.11	-10.89	9.43	-13.59
Bn	15.52	6.02	12.87	-6.52	10.62	-14.15
OPh	13.78	4.96	11.56	-12.76	9.29	-11.66
OBn	14.73	4.24	12.95	-12.16	8.09	-12.09

Figure 3. Transition states involved in the Steglich rearrangement of isoxazolones. The values in parenthesis corresponds to the atom distances in the molecular complexes right before and after the transition states

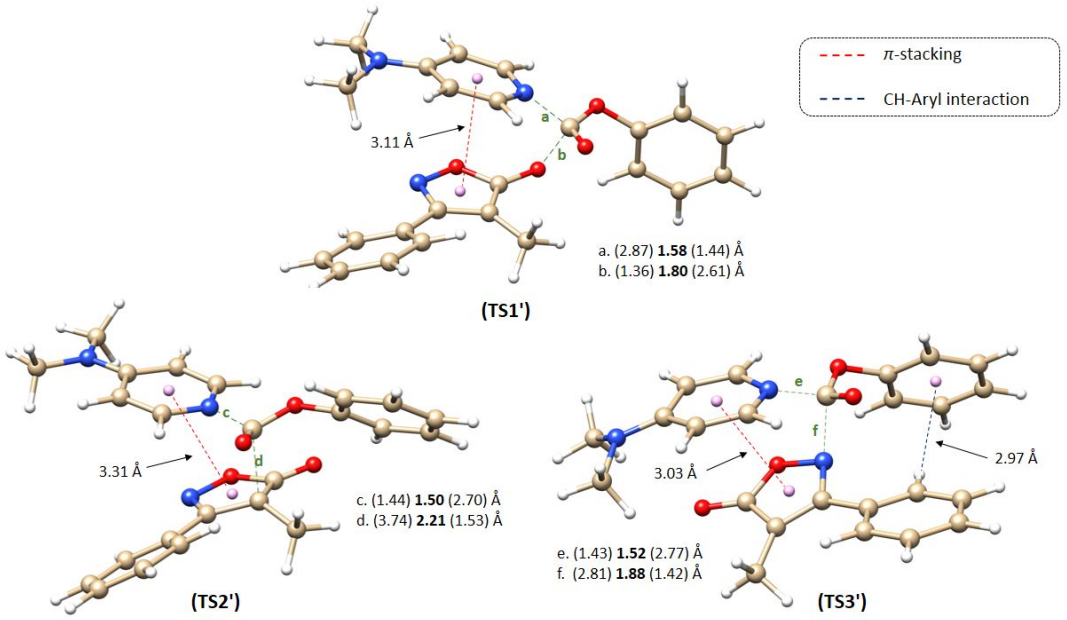

From this molecular complex (MC2'), the reaction can proceed to products **7** or **8**. In both cases π-stacking interactions between the isoxazolone moiety and the DMAP pyridine ring

were found, as well as a CH-aryl interaction in TS3' (Figure 3). The considerable differences in the barriers (12-14 kcal/mol for TS2' and 9-11 kcal/mol for TS3' suggest that adduct **8** be kinetic favored during the reaction course and, therefore, could be selectively isolated at lower temperatures (Figure 4). On the other hand, thermodynamic seems to play a minor role (especially for acyloxy groups), in some cases driving the reaction towards **7** and in others towards **8**, without great selectivity.

Figure 4. Reaction pathway for the formation of products 7 and 8 (R = OPh)

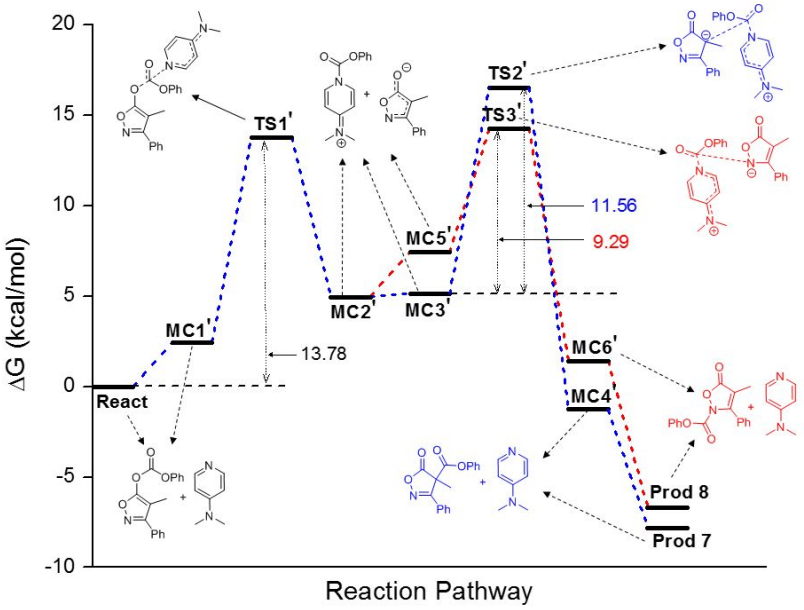

A key consideration must be evoked to allow the selective access to **7**: while in product **7** the C---C bond is irreversible formed, the carbamate group formed in adduct **8** is susceptible to DMAP nucleophilic attack ($\Delta G^{\ddagger}$ = 20.95 kcal/mol), restoring the ion-pairing intermediate. Over time, this would allow the selective access to **7**. It is worth mentioning that this would only be viable if enough energy is provided, thus requiring heating of the reaction mixture.

To sum up, at lower temperatures the kinetic product **8** would be accessed and at higher temperatures reaction reversibility starts to play a key role and therefore allows the formation

of **7**. To test these hypotheses, we decided to carry out the experimental Steglich rearrangement of isoxazolones based on computational findings. The desired precursors (**13a-e**) were prepared employing a four steps protocol (Scheme 4), which included: 1) oxime formation/intramolecular cyclization; 2) Knoevenagel condensation with different aldehydes; 3) double-bond reduction; 4) *O*-acyloxylation.

Scheme 4. Preparation of intermediates 13a-e

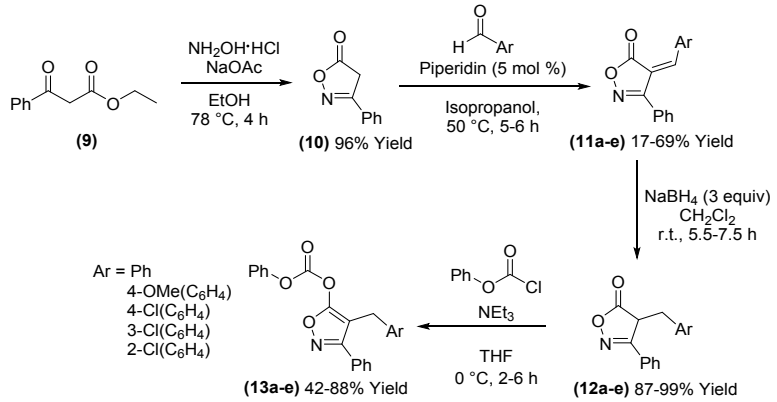

Next, the Steglich rearrangement was carried out at -25 °C, room temperature (≈25 °C) and 90 °C to check if our hypothesis is plausible to experimentally occur (full details concerning the reaction optimization are available in the SI). We observed that at room temperature both products (**14** and **15**) are formed without selectivity and in near a 1:1 ratio. The reaction at -25 °C selectively afforded the desired adducts **15a-d**, although, in this case, longer reaction times were required to complete consumption of the starting material (Scheme 5). Particularly, the kinetic control perfect explains the reaction selectivity towards this site. Most interesting, the heating of the reaction completely inverted the regioselectivity, affording only products **14a-e** in moderate to good yields after less than an hour. These results are also in good agreement with our prediction, suggesting that indeed the reversibility of **15** seem to be involved.

Scheme 5. Reaction scope towards both reactive sites

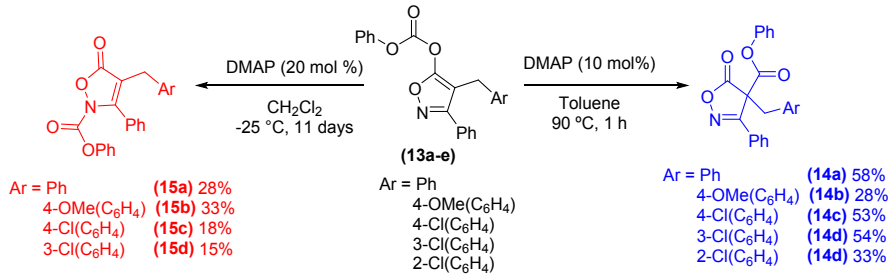

Finally, a control experiment was carried out to validate our hypothesis of reaction reversibility (Scheme 6). To this purpose, product **15a** was employed as substrate in the presence of catalytic DMAP, toluene as solvent, at 90 °C. With this process, we aimed to detect either **13a** and/or **14a** after a few minutes, indicating that the ion-pairing intermediate can be formed through the adduct **15a**. To our delight, we observed the formation of product **13a** (full details concerning this control experiment are available in the SI).

Scheme 6. Reaction reversibility investigation.

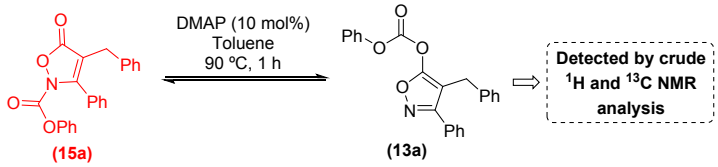

CONCLUSIONS

In summary, the theoretical evaluation of the Steglich rearrangement of azlactones, aiming to get new insights towards the reaction regioselectivity has been presented. The data revealed that the C4 products are kinetic and thermodynamic favored over the C2 adduct. The drastic enhancement in the steric hindrance inverted the reactivity and allowed the access to C2 product. The use of the same model in isoxazolones allowed the prediction of the reactivity of these cycles, based on kinetic control or reaction reversibility as driving factors. These

computational findings allowed the first experimental report on the highly regioselective Steglich rearrangement of isoxazolones, rendering both N2 and C4 adducts in moderate to good yields.

EXPERIMENTAL SECTION

General Remarks. All purchased chemicals were employed without further purification. Solvents were dried according to standard procedures. Thin layer chromatography (TLC) was performed on TLC plates (silica gel 60 F_{254}) and visualized by a UV lamp; column chromatography was performed using 230− 400 mesh silica gel. Yields refer to chromatographically purified and spectroscopically pure compounds. The ^{1}H and ^{13}C NMR spectra were recorded at 500 MHz and 125 MHz, respectively. Chemical shifts for ^{1}H and ^{13}C NMR were reported as δ (parts per million) relative to the signals of $CHCl_3$ at 7.26 ppm (singlet) and 77 ppm (triplet), respectively. Chemical shifts are reported employing the following peak abbreviations pattern: br, broad; s, singlet; d, doublet; dd, double doublet; t, triplet; dt, double triplet; q, quartet; pent, pentet; sext, sextet; m, multiplet. High resolution mass spectra were acquired in the positive ion mode using a time-of-flight (TOF) mass spectrometer equipped with an ESI source. Melting points were recorded on a melting point apparatus.

General Method for the Synthesis of *3-phenylisoxazol-5(4H)-one* (10)

3-phenylisoxazol-5(4H)-one was prepared according to the literature method[15] and obtained as a violet solid (3.506 g, 96%).

General procedure for the synthesis of condensed compounds (11a-e)

Condensed compounds were prepared according to the literature method.[15]

(Z)-4-(benzylidene)-3-phenylisoxazol-5(4H)-one (**11a**).[15] This compound was isolated by filtration as a yellow solid (3.54 g, 69%).

(Z)-4-(4-methoxybenzylidene)-3-phenylisoxazol-5(4H)-one (**11b**).[30] This compound was isolated by filtration as a yellow solid (1.76 g, 68%).

(Z)-4-(4-chlorobenzylidene)-3-phenylisoxazol-5(4H)-one (**11c**).[31] This compound was isolated by filtration as a yellow solid (1.63 g, 62%).

(Z)-4-(3-chlorobenzylidene)-3-phenylisoxazol-5(4H)-one (**11d**). This compound was isolated by flash chromatography on silica gel (Hexanes: EtOAc = 9:1) as an orange solid (0.45 g, 17%). Mp: 135.1-136.0 °C. FT-IR (NaCl, cm^{-1}) ν 3103, 3065, 2914, 1757, 1617, 1117, 1097. ^{1}H NMR (500 MHz, $CDCl_3$) δ: 8.26-8.24 (m, 2H), 7.60-7.53 (m, 7H), 7.45 (t, 1H, *J* = 7.8 Hz). ^{13}C $\{^{1}H\}$ NMR (125 MHz, $CDCl_3$) δ: 167.8, 163.9, 150.8, 148.9, 135.1, 133.9, 133.8, 132.1, 131.8, 131.7, 131.3, 131.0, 130.3, 130.0, 129.6, 128.8, 128.2, 127.1, 120.4. HRMS (ESI-TOF) *m/z*: $[M+H]^+$ calcd for $C_{16}H_{11}ClNO_2$ 284.0478, found 284.0467.

(Z)-4-(2-chlorobenzylidene)-3-phenylisoxazol-5(4H)-one (**11e**).[15] This compound was isolated by flash chromatography on silica gel (Hexanes: EtOAc = 9:1) as a yellow solid (0.97 g, 37%).

General procedure for the synthesis of reduced compounds (12a-e)

The corresponding condensed product (3.52 mmol, 1.0 equiv.) was dissolved in 40.0 mL of CH_2Cl_2 and then $NaBH_4$ (10.5 mmol, 3.0 equiv.) was added, in small portions. The resultant solution was stirred at room temperature and monitored by TLC analysis (reaction time between 5.5 and 7.5 hours). After the reaction was complete, the mixture was treated with a 9% aqueous HCl solution. Then, the organic phase was separated and the aqueous phase extracted once more

with CH_2Cl_2. The combined organic phases were dried with anhydrous Na_2SO_4, filtered and concentrated under reduced pressure. The resulting crude material was employed in the next reaction step without further purification and were obtained as a mixture of imine/enamine tautomers.

4-benzyl-3-phenylisoxazol-5(4H)-one (**12a**).[31] The product was obtained as a yellow solid (0.98 g, 87%). Reaction time: 5.5 h. Mp: 104.2-105.0 °C. FT-IR (NaCl, cm^{-1}) ν 3062, 3029, 2912, 2849, 1798, 1693, 1612, 1029. ^{1}H NMR (500 MHz, $CDCl_3$) δ: 7.60-7.39 (m, 7.7H), 7.27-7.15 (m, 5.7H), 6.87 (dd, 1H, *J* = 1.65, 1.3 Hz), 4.15 (dd, 0.95H, *J* = 5.6, 4.8 Hz), 3.76 (s, 0.7H), 3.37 (dd, 1H, *J* = 14.1, 4.8 Hz), 3.29 (dd, 1H, *J* = 14.1, 5.6 Hz). ^{13}C {^{1}H} NMR (125 MHz, $CDCl_3$) δ: 171.7, 173.9, 165.9, 162.9, 138.9, 134.4, 131.9, 131.5, 129.4, 129.3, 129.1, 128.7, 128.2, 127.8, 127.7, 127.6, 127.1, 126.5, 102.1, 46.6, 34.8, 28.2.

4-(4-methoxybenzyl)-3-phenylisoxazol-5(4H)-one (**12b**).[31] The product was obtained as a yellow solid (1.285 g, 98 %). Reaction time: 7 h. Mp: 110.9-111.8 °C. FT-IR (NaCl, cm^{-1}) ν 3064, 2932, 2835, 1797, 1694, 1612, 1513, 1246, 1033. ^{1}H NMR (500 MHz, $CDCl_3$) δ: 7.62-7.60 (m, 1.99H), 7.57-7.54 (m, 1.04H), 7.51-7.44 (m, 3.14H), 7.17-7.14 (m, 0.46H), 6.81-6.76 (m, 2.47H), 6.70-6.67 (m, 1.97H), 4.12-4.10 (m, 0.95H), 3.76-3.73 (m, 4.26H), 3.33 (dd, 1.01H, *J* = 14.2, 4.6 Hz), 3.24 (dd, 1H, *J* = 14.2, 5.4 Hz). ^{13}C {^{1}H} NMR (125 MHz, $CDCl_3$) δ: 177.8, 173.7, 165.9, 162.8, 159.1, 158.3, 132.0, 131.5, 130.3, 129.4, 129.2, 127.9, 127.7, 127.1, 126.3, 114.2, 114.1, 103.4, 55.4, 55.3, 46.9, 34.0, 27.4.

4-(4-chlorobenzyl)-3-phenylisoxazol-5(4H)-one (**12c**).[31] The product was obtained as a yellow solid (0.977 g, 97 %). Reaction time: 5.5 h. Mp: 115.5-116.6 °C. FT-IR (NaCl, cm^{-1}) ν 3065, 2814, 1796, 1694, 1614, 1491, 1014. ^{1}H NMR (500 MHz, $CDCl_3$) δ: 7.60-7.55 (m, 3.2H), 7.52-7.49 (m, 2.5H), 7.47-7.46 (m, 1.7H), 7.23-7.21 (m, 0.95H), 6.80-6.78 (m, 1.9H), 4.15 (dd, 0.98H, *J* = 5.4, 4.8

Hz), 3.71 (s, 0.84H), 3.51 (dd, 1.06H, *J* = 14.1, 4.6 Hz), 3.25 (dd, 1H, *J* = 14.2, 5.6 Hz). ^{13}C {^{1}H} NMR (125 MHz, $CDCl_3$) δ: 177.5, 173.7, 165.6, 163.0, 137.3, 135.3, 133.9, 132.8, 132.4, 132.2, 131.7, 130.6, 129.6, 129.5, 128.9, 128.8, 127.7, 127.6, 127.2, 127.0, 101.9, 46.5, 34.1, 27.6.

4-(3-chlorobenzyl)-3-phenylisoxazol-5(4H)-one (**12d**). The product was obtained as a red oil (0.453 g, 99 %). Reaction time: 7.5 h. FT-IR (NaCl, cm^{-1}) ν 3063, 2820, 1798, 1692, 1611, 1474, 1431, 1044. ^{1}H NMR (500 MHz, $CDCl_3$) δ: 7.59-7.55 (m,3H), 7.53-7.49 (m, 2.7H), 7.47-7.46 (m, 2.1H), 7.20-7.16 (m, 3.09H), 7.13-7.10 (1.59H), 6.81-6.79 (m, 1.83H), 4.18 (dd, 0.91H, *J* = 5.7, 4.7 Hz), 3.75 (s, 1.14H), 3.35 (dd, 1.08H, *J* = 14.1, 4.7 Hz), 3.26 (dd, 1H, *J* = 14.1, 5.7 Hz). ^{13}C {^{1}H} NMR (125 MHz, $CDCl_3$) δ: 177.4, 173.7, 165.7, 163.1, 140.9, 136.4, 134.5, 132.2, 131.7, 130.1, 130.0, 129.6, 129.5, 129.4, 128.3, 128.1, 127.7, 127.6, 127.3, 127.1, 126.9, 126.4, 46.4, 34.3, 27.9. HRMS (ESI-TOF) *m/z*: $[M+Na]^+$ calcd for $C_{16}H_{12}ClNNaO_2$ 308.0454, found 308.0439.

4-(2-chlorobenzyl)-3-phenylisoxazol-5(4H)-one (**12e**).[32] The product was obtained as a pink solid (0.182 g, 95 %). Reaction time: 5.5 h. Mp: 113.2-114.9 °C. FT-IR (NaCl, cm^{-1}) ν 3067, 2927, 2817, 1801, 1695, 1613, 1445, 1050. ^{1}H NMR (500 MHz, $CDCl_3$) δ: 7.57-7.55 (m 2H), 7.49-7.46 (m, 1.75H), 7.43-7.42 (m, 2.15H), 7.40-7.37 (m, 2.14H), 7.35-7.33 (m, 1.5H), 7.24-7.19 (m, 1.6H), 7.17-7.14 (m, 1H), 7.13-7.06 (m, 1.9H), 4.25 (dd, 0.90H, *J* = 6.7, 8.5 Hz), 3.87 (s, 1H), 3.40 (dd, 0.95H, *J* = 14.2, 6.7 Hz), 3.21 (dd, 1H, *J* = 14.2, 8.5 Hz). ^{13}C {^{1}H} NMR (125 MHz, $CDCl_3$) δ: 177.0, 173.5, 166.7, 163.6, 134.1, 132.7, 132.3, 131.9, 131.7, 129.8, 129.6, 129.5, 129.4, 129.3, 129.2, 128.0, 127.6, 127.5, 127.3, 127.2, 127.1, 101.0, 43.7, 33.8, 26.0.

General procedure for the synthesis of isoxazolone carbonates (13a-e)

Isoxazolone carbonates **13a-e** were prepared by adapting a methodology described for azlactone enol carbonate synthesis.[9] To a solution of a reduced intermediate (12a-e) (2.1 mmol, 1.0 equiv.) in THF (18.0 mL, 8.5 mL/mmol of intermediate) at 0 °C, Et_3N (2.3 mmol, 1.1 equiv.)

and phenyl chloroformate (2.3 mmol, 1.1 equiv.) were added, with the formation of a white precipitate. The resulting mixture was stirred at 0 °C, until no starting material was detected by TLC (reaction time between 2 and 6 hours). Then, the reaction was washed with H_2O and extracted with Et_2O (2x). The combined organic phases were washed with 0.1 M aqueous HCl solution, 0.1 M aqueous $NaHCO_3$ solution and brine. Then, it was dried with anhydrous Na_2SO_4, filtered and concentrated under reduced pressure. The residue was purified through flash chromatography on silica gel (Hexanes: EtOAc = 95:5 to 80:20) or recrystallization in Hexanes.

4-benzyl-3-phenylisoxazol-5-yl phenyl carbonate (**13a**). This compound was isolated by recrystallization as a white solid (0.58 g, 74%). Reaction time: 2 h. Mp: 100.6-101.9 °C. FT-IR (NaCl, cm^{-1}) ν 3062, 3030, 2914, 1776, 1751, 1333, 1212. ^{1}H NMR (500 MHz, $CDCl_3$) δ: 7.55-7.49 (m, 3H), 7.47-7.45 (m, 2H), 7.38-7.35 (m, 2H), 7.33-7.28 (m, 2H), 7.27-7.21 (m, 4H), 7.22-7.21 (m, 2H), 3.65 (s, 2H). ^{13}C {^{1}H} NMR (125 MHz, $CDCl_3$) δ: 167.4, 156.6, 149.8, 146.2, 137.9, 129.7, 128.8, 128.7, 128.6, 128.4, 126.9, 120.9, 109.0, 28.3. HRMS (ESI-TOF) *m/z*: $[M+Na]^+$ calcd for $C_{23}H_{17}NNaO_4$ 394.1055, found 394.1047.

4-(4-methoxybenzyl)-3-phenylisoxazol-5-yl phenyl carbonate (**13b**). This compound was isolated by flash chromatography (Hexanes: EtOAc = 90:10) as a white solid (0.69 g, 42%). Reaction time: 6 h. Mp: 118.6-119.5 °C. FT-IR (NaCl, cm^{-1}) ν 3064, 2911, 2837 1775, 1752, 1513, 1209. ^{1}H NMR (500 MHz, $CDCl_3$) δ: 7.54-7.47 (m, 3H), 7.45-7.42 (m, 2H), 7.35-7.32 (m, 2H), 7.24-7.21 (m, 1H), 7.10-7.07 (m, 4H), 6.82-6.81 (m, 1H), 3.78 (s, 3H), 3.55 (s, 2H). ^{13}C {^{1}H} NMR (125 MHz, $CDCl_3$) δ: 167.5, 158.5, 156.4, 149.8, 146.2, 131.0, 130.0, 129.7, 129.5, 128.8, 128.7, 127.5, 126.7, 120.9, 114.2, 109.4, 55.4, 27.4. HRMS (ESI-TOF) *m/z*: $[M+Na]^+$ calcd for $C_{24}H_{19}NNaO_5$ 424.1161, found 424.1148.

4-(4-chlorobenzyl)-3-phenylisoxazol-5-yl phenyl carbonate (**13c**). This compound was isolated by recrystallization as a white solid (1.49 g, 88%). Reaction time: 4 h. Mp: 119.9-121.2 °C. FT-IR (NaCl, cm^{-1}) ν 3065, 2922, 2853, 1773, 1750, 1493, 1339, 1214. ^{1}H NMR (500 MHz, $CDCl_3$) δ: 7.54-7.51 (m, 1H), 7.50-7.47 (m, 2H), 7.42-7.39 (m, 2H), 7.35-7.31 (m, 2H), 7.25-7.21 (m, 3H), 7.10-7.07 (m, 4H), 3.57 (s, 2H). ^{13}C {^{1}H} NMR (125 MHz, $CDCl_3$) δ: 167.3, 156.8, 149.8, 146.1, 136.4, 131.2, 129.8, 129.7, 128.9, 128.8, 128.7, 126.8, 120.9, 108.5, 27.7. HRMS (ESI-TOF) *m/z*: $[M+Na]^+$ calcd for $C_{23}H_{16}ClNNaO_4$ 428.0666, found 428.0658.

4-(3-chlorobenzyl)-3-phenylisoxazol-5-yl phenyl carbonate (**13d**). This compound was isolated by flash chromatography (Hexanes: EtOAc = 95:5 to 80:20) as a pink solid (0.35 g, 62%). Reaction time: 2 h. Mp: 101.4-102.3 °C. FT-IR (NaCl, cm^{-1}) ν 3065, 2926, 1775, 1752, 1344, 1307, 1213. ^{1}H NMR (500 MHz, $CDCl_3$) δ: 7.52-7.47 (m, 3H), 7.41-7.39 (m, 2H), 7.35-7.32 (m, 2H), 7.24-7.21 (m, 1H), 7.20-7.19 (m, 2H), 7.11-7.07 (m, 3H), 7.06-7.04 (m, 1H), 3.58 (s, 2H). ^{13}C {^{1}H} NMR (125 MHz, $CDCl_3$) δ: 167.2, 156.9, 149.8, 139.9, 131.2, 130.1, 129.7, 128.8, 128.6, 128.5, 127.2, 127.1, 126.8, 126.6, 120.9, 108.2, 27.9. HRMS (ESI-TOF) *m/z*: $[M+Na]^+$ calcd for $C_{23}H_{16}ClNNaO_4$ 428.0666, found 428.0665.

4-(2-chlorobenzyl)-3-phenylisoxazol-5-yl phenyl carbonate (**13e**). This compound was isolated by recrystallization as a white solid (0.20 g, 77%). Reaction time: 4 h. Mp: 100.3-101.9 °C. FT-IR (NaCl, cm^{-1}) ν 3063, 3021, 2921, 1777, 1752, 1630, 1346, 1312, 1213. ^{1}H NMR (500 MHz, $CDCl_3$) δ: 7.48-7.45 (m 1H), 7.43-7.40 (m, 2H), 7.38-7.32 (m, 4H), 7.30-7.29 (m, 1H), 7.30 (m, 1H), 7.24-7.21 (m, 2H), 7.19-7.13 (m, 2H), 7.11-7.09 (m, 2H), 3.76 (s, 2H). ^{13}C {^{1}H} NMR (125 MHz, $CDCl_3$) δ: 167.2, 157.4, 149.9, 146.1, 131.0, 130.2, 129.7, 129.6, 128.7, 128.6, 128.3, 127.0, 126.8, 120.9, 107.2, 26.2. HRMS (ESI-TOF) *m/z*: $[M+Na]^+$ calcd for $C_{23}H_{16}ClNNaO_4$ 428.0666, found 428.0658.

General procedures for the synthesis of compounds 14a-e

To a solution of the corresponding isoxazolone carbonates (13a-e) (0.13 mmol, 1.0 equiv.) in 1.0 mL of toluene at 90 °C, 10 mol% of DMAP (0.013 mmol, 0.1 equiv.) was added. The reaction mixture was stirred at 90 °C in an oil bath for 1 h (monitored by TLC analysis). After that, the mixture was cooled to room temperature and treated with 10.0 mL of 0.1 M aqueous HCl solution. The organic phase was separated and concentrated under reduced pressure. The crude Steglich rearrangement products were purified through flash chromatography on silica gel (Hexanes: EtOAc = 9:1).

Phenyl-4-benzyl-5-oxo-3-phenyl-4,5-dihydroisoxazole-4-carboxylate (**14a**). This compound was isolated as a colorless oil (29 mg, 58%). FT-IR (NaCl, cm^{-1}) ν 3067, 3032, 2929, 1803, 1765, 1589, 1493 1180. ^{1}H NMR (500 MHz, $CDCl_3$) δ: 7.78-7.76 (m, 2H), 7.72-7.70 (m, 1H), 7.57-7.54 (m, 2H), 7.39-7.35 (m, 2H), 7.28-7.27 (m, 1H), 7.25-7.22 (m, 1H), 7.19-7.16 (m, 2H), 7.01-6.99 (m, 2H), 6.88-6.86 (m, 2H), 3.77 (d, 1H, *J* = 14.1 Hz), 3.70 (d, 1H, *J* = 14.1 Hz).^{13}C {^{1}H} NMR (125 MHz, $CDCl_3$) δ: 174.4, 163.9, 163.1, 150.0, 132.6, 131.9, 129.8, 129.8, 129.7, 128.8, 128.3, 127.4, 127.1, 126.7, 120.9, 62.7, 38.5. HRMS (ESI-TOF) *m/z*: $[M+Na]^+$ calcd for $C_{23}H_{17}NNaO_4$ 394.1055, found 394.1047.

Phenyl-4-(4-methoxybenzyl)-5-oxo-3-phenyl-4,5-dihydroisoxazole-4-carboxylate (**14b**). This compound was isolated as a colorless oil (15 mg, 28%). FT-IR (NaCl, cm^{-1}) ν 3044, 2935, 2838, 1800, 1763, 1612, 1513, 1446, 1254, 1179. ^{1}H NMR (500 MHz, $CDCl_3$) δ: 7.78-7.77 (m, 2H), 7.63-7.60 (m, 1H), 7.56-7.53 (m, 2H), 7.38-7.34 (m, 2H), 7.27-7.24 (m, 1H), 7.00-6.98 (m, 2H), 6.80-6.78 (m, 2H), 6.70-6.69 (m, 2H), 3.74 (s, 3H), 3.73 (d, 1H, *J* = 14.2 Hz), 3.65 (d, 1H, *J* = 14.2 Hz). ^{13}C {^{1}H} NMR (125 MHz, $CDCl_3$) δ: 174.4, 163.9, 163.2, 159.5, 150.0, 132.5, 130.8, 129.8, 129.7, 127.4, 127.0, 126.7, 123.8, 120.9, 114.2, 62.8, 55.3, 37.8. HRMS (ESI-TOF) *m/z*: $[M+Na]^+$ calcd for $C_{24}H_{19}NNaO_5$ 424.1161, found 424.1155.

Phenyl-4-(4-chlorobenzyl)-5-oxo-3-phenyl-4,5-dihydroisoxazole-4-carboxylate (**14c**). This compound was isolated as a colorless oil (28 mg, 53%). FT-IR (NaCl, cm^{-1}) ν 3065, 2922, 2853, 1803, 1765, 1589, 1493, 1228, 1181. ^1H NMR (500 MHz, $CDCl_3$) δ: 7.74-7.72 (m, 2H), 7.61-7.58 (m, 1H), 7.54-7.51 (m, 2H), 7.40-7.32 (m, 2H), 7.25-7.22 (m, 1H), 7.13-7.11 (m, 2H), 6.97-6.95 (m, 2H), 6.78-6.76 (m, 2H), 3.69 (d, 1H, *J* = 14.2 Hz), 3.63 (d, 1H, *J* = 14.2 Hz). ^{13}C {^1H} NMR (125 MHz, $CDCl_3$) δ: 174.2, 163.7, 162.9, 152.2, 151.1, 150.0, 134.4, 132.7, 131.0, 130.5, 129.9, 129.8, 129.7, 129.1, 127.2, 127.1, 126.6, 126.4, 121.0, 120.9, 62.5, 37.8. HRMS (ESI-TOF) *m/z*: $[M+Na]^+$ calcd for $C_{23}H_{16}ClNNaO_4$ 428.0666, found 428.0657.

Phenyl-4-(3-chlorobenzyl)-5-oxo-3-phenyl-4,5-dihydroisoxazole-4-carboxylate (**14d**). This compound was isolated as a colorless oil (29 mg, 54%). FT-IR (NaCl, cm^{-1}) ν 3065, 2930, 1800, 1764, 1598, 1492, 1204, 1183. ^1H NMR (500 MHz, $CDCl_3$) δ: 7.76-7.73 (m, 2H), 7.65-7.62 (m, 1H), 7.58-7.55 (m, 2H), 7.39-7.36 (m, 2H), 7.29-7.27 (m, 1H), 7.23-7.21 (m, 1H), 7.14-7.11 (m, 1H), 7.02-7.00 (m, 2H), 6.80 (d, 1H, *J* = 7.7 Hz), 6.77 (t, 1H, *J* = 1.7 Hz), 3.71 (d, 1H, *J* = 14.1 Hz), 3.64 (d, 1H, *J* = 14.1 Hz). ^{13}C {^1H} NMR (125 MHz, $CDCl_3$) δ: 174.1, 163.6, 162.9, 150.0, 134.6, 133.9, 132.8, 130.2, 129.9, 129.8, 128.6, 127.8, 127.2, 127.1, 126.7, 120.9, 62.4, 37.9. HRMS (ESI-TOF) *m/z*: $[M+Na]^+$ calcd for $C_{23}H_{16}ClNNaO_4$ 428.0666, found 428.0666.

Phenyl-4-(2-chlorobenzyl)-5-oxo-3-phenyl-4,5-dihydroisoxazole-4-carboxylate (**14e**). This compound was isolated as a yellow oil (18 mg, 33%). FT-IR (NaCl, cm^{-1}) ν 3066, 2925, 2850, 1803, 1765, 1592, 1493, 1231, 1179. ^1H NMR (500 MHz, $CDCl_3$) δ: 7.69-7.68 (m, 2H), 7.54-7.51 (m, 1H), 7.46-7.42 (m, 2H), 7.40-7.37 (m, 2H), 7.35-7.32 (m, 2H), 7.25-7.22 (m, 2H), 7.20-7.18 (m, 1H), 7.15-7.10 (m, 1H), 6.96-6.95 (m, 1H), 3.96 (d, 1H, *J* = 14.6 Hz), 3.90 (d, 1H, *J* = 14.6 Hz). ^{13}C {^1H} NMR (125 MHz, $CDCl_3$) δ: 174.1, 164.0, 163.5, 151.1, 150.0, 135.1, 132.4, 131.6, 130.5, 130.0, 129.8, 129.7, 129.6, 129.5, 127.3, 127.2, 127.1, 126.9, 126.4, 121.1, 120.9, 61.5, 34.8. HRMS (ESI-TOF) *m/z*: $[M+Na]^+$ calcd for $C_{23}H_{16}ClNNaO_4$ 428.0666, found 428.0659.

General procedures for the synthesis of compounds 15a-d

To a solution of the corresponding isoxazolone carbonates (13a-d) (0.13 mmol, 1.0 equiv.) in 1.0 mL of toluene, 20 mol% of DMAP (0.026 mmol, 0.2 equiv.) was added. The reaction mixture was maintained at -25 °C for 11 days (monitored by TLC analysis). The mixture was then treated with 10.0 mL of 0.1 M aqueous HCl solution. The organic phase was separated and concentrated under reduced pressure. The crude reaction mixtures were purified through flash chromatography on silica gel (Hexanes: EtOAc = 9: 1).

Phenyl-4-benzyl-5-oxo-3-phenylisoxazole-2(5H)-carboxylate (**15a**). This compound was isolated as a colorless oil (14 mg, 28%). FT-IR (NaCl, cm^{-1}) ν 3066, 3034, 2921, 2850, 1810, 1767, 1494, 1262, 1086. ^{1}H NMR (500 MHz, $CDCl_3$) δ: 7.89-7.88 (m, 2H), 7.61-7.52 (m, 1H), 7.55-7.52 (m, 2H), 7.36-7.33 (m, 2H), 7.28-7.27 (m, 1H), 7.24-7.20 (m, 3H), 7.12-7.10 (m, 2H), 6.96-6.94 (m, 2H), 3.60 (d, 1H, *J* = 13.2 Hz), 3.56 (d, 1H, *J* = 13.2 Hz). ^{13}C $\{^{1}H\}$ NMR (125 MHz, $CDCl_3$) δ: 173.4, 161.2, 151.2, 150.7, 132.6, 130.4, 129.8, 129.7, 129.4, 129.2, 128.9, 128.7, 126.9, 126.6, 126.5, 120.6, 82.4, 41.5. HRMS (ESI-TOF) *m/z*: $[M+H]^+$ calcd for $C_{23}H_{17}NNaO_4$ 394.1055, found 394.1049.

Phenyl-4-(4-methoxybenzyl)-5-oxo-3-phenylisoxazole-2(5H)-carboxylate (**15b**). This compound was isolated as a colorless oil (18 mg, 33%). FT-IR (NaCl, cm^{-1}) ν 3035, 2932, 2838, 1812, 1768, 1614, 1514, 1255, 1085. ^{1}H NMR (500 MHz, $CDCl_3$) δ: 7.91-7.89 (m, 2H), 7.61-7.58 (m, 1H), 7.55-7.52 (m, 2H), 7.36-7.32 (m, 2H), 7.25-7.22 (m, 1H), 7.12-7.10 (m, 2H), 6.87-6.85 (m, 2H), 6.75-6.72 (m, 2H), 3.75 (s, 3H), 3.55 (d, 1H, *J* = 13.4 Hz), 3.51 (d, 1H, *J* = 13.4 Hz). ^{13}C $\{^{1}H\}$ NMR (125 MHz, $CDCl_3$) δ: 173.5, 161.3, 159.8, 151.3, 150.7, 132.6, 131.5, 130.6, 129.8, 129.7, 129.0, 128.7, 128.1, 126.9, 126.6, 120.9, 120.6, 114.3, 114.2, 113.9, 82.4, 55.3, 40.7. HRMS (ESI-TOF) *m/z*: $[M+H]^+$ calcd for $C_{24}H_{19}NNaO_5$ 424.1161, found 424.1155.

Phenyl-4-(4-chlorobenzyl)-5-oxo-3-phenylisoxazole-2(5H)-carboxylate (**15c**). This compound was isolated as a colorless oil (10 mg, 18%). FT-IR (NaCl, cm^{-1}) ν 3063, 2925, 2852, 1811, 1765, 1492, 1263, 1087. ^{1}H NMR (500 MHz, $CDCl_3$) δ: 7.90-7.87 (m, 2H), 7.63-7.59 (m, 1H), 7.56-7.53 (m, 2H), 7.37-7.32 (m, 2H), 7.24-7.23 (m, 1H), 7.21-7.18 (m, 2H), 7.12-7.10 (m, 2H), 6.90-6.87 (m, 2H), 3.55 (d, 1H, *J* = 13.4 Hz), 3.52 (d, 1H, *J* = 13.4 Hz). ^{13}C $\{^{1}H\}$ NMR (125 MHz, $CDCl_3$) δ: 173.1, 161.1, 151.2, 150.7, 134.9, 132.7, 131.7, 129.8, 129.7, 129.1, 127.7, 127.0, 126.5, 126.4, 120.6, 82.0, 40.8. HRMS (ESI-TOF) *m/z*: $[M+H]^+$ calcd for $C_{23}H_{16}ClNNaO_4$ 428.0666, found 428.0661.

Phenyl-4-(3-chlorobenzyl)-5-oxo-3-phenylisoxazole-2(5H)-carboxylate (**15d**). This compound was isolated as a colorless oil (8 mg, 15%). FT-IR (NaCl, cm^{-1}) ν 3067, 2925, 2853, 1811, 1768, 1598, 1493, 1265, 1089. ^{1}H NMR (500 MHz, $CDCl_3$) δ: ^{13}C $\{^{1}H\}$ NMR (125 MHz, $CDCl_3$) δ: 7.88-7.86 (m, 2H), 7.63-7.60 (m, 1H), 7.57-7.53 (m, 2H), 7.37-7.33 (m, 2H), 7.27-7.23 (m, 2H), 7.18-7.15 (m, 1H), 7.13-7.11 (m, 2H), 6.90-6.87 (m, 2H), 3.52 (br, 2H). ^{13}C $\{^{1}H\}$ NMR (125 MHz, $CDCl_3$) δ: 173.0, 161.1, 151.2, 150.7, 134.6, 132.8, 131.2, 130.5, 130.1, 129.8, 129.7, 129.0, 128.6, 127.0, 126.5, 126.4, 120.6, 81.9, 40.9. HRMS (ESI-TOF) *m/z*: $[M+H]^+$ calcd for $C_{23}H_{16}ClNNaO_4$ 428.0666, found 428.0663.

ASSOCIATED CONTENT

- Supporting Information

Reaction optimization data, reaction reversibility study, copies of ^{1}H NMR, ^{13}C NMR, and IR spectra for all compounds, Molecular complexes structures, Cartesian coordinates and total energy data for all stationary points on the potential energy surface.

AUTHOR INFORMATION

- Corresponding Authors

* helio.santos@ufjf.edu.br

* giovanni.amarante@ufjf.edu.br

- ORCID

Pedro Pôssa de Castro: 0000-0002-3018-3130

Giovanni Wilson Amarante: 0000-0003-1004-5395

- Notes

The authors declare no competing financial interest.

ACKNOWLEDGEMENTS

We are grateful for generous financial support from CAPES (Finance Code 001), CNPq, FAPEMIG, and Rede Mineira de Química. Furthermore, we are grateful to Beatriz Rocha de Moraes (Chemistry Department/UFJF) for helpful contributions concerning the IR analyses and Prof. Giuliano Clososki and Thiago Santos (FCFRP-USP) for all their help with HRMS analyses. We thank Dr. Danielle Pinheiro for initial studies.

REFERENCES

(1) Ravelli, D.; Protti, S.; Fagnoni, M. Carbon–Carbon Bond Forming Reactions via Photogenerated Intermediates. *Chem. Rev.* **2016**, *116* (17), 9850–9913. https://doi.org/10.1021/acs.chemrev.5b00662.

(2) Eppe, G.; Didier, D.; Marek, I. Stereocontrolled Formation of Several Carbon–Carbon Bonds in Acyclic Systems. *Chem. Rev.* **2015**, *115* (17), 9175–9206. https://doi.org/10.1021/cr500715t.

(3) Steglich, W.; Höfle, G. 5-Acyloxyoxazoles and Their Rearrangement to 4-Acyloxazol-5-Ones. *Angew. Chem. Int. Ed. English* **1968**, *7* (1), 61–61. https://doi.org/10.1002/anie.196800611.

(4) Fujii, K.; Mitsudo, K.; Mandai, H.; Korenaga, T.; Suga, S. Enantioselective Acyl Migration Reactions of Furanyl Carbonates with Chiral DMAP Derivatives. *Chem. Eur. J.* **2018**, chem.201806050. https://doi.org/10.1002/chem.201806050.

(5) Campbell, C. D.; Joannesse, C.; Morrill, L. C.; Philp, D.; Smith, A. D. Regiodivergent Lewis Base-Promoted O- to C-Carboxyl Transfer of Furanyl Carbonates. *Org. Biomol. Chem.* **2015**, *13* (10), 2895–2900. https://doi.org/10.1039/C4OB02629B.

(6) Mandai, H.; Fujii, K.; Yasuhara, H.; Abe, K.; Mitsudo, K.; Korenaga, T.; Suga, S. Enantioselective Acyl Transfer Catalysis by a Combination of Common Catalytic Motifs and Electrostatic Interactions. *Nat. Commun.* **2016**, *7* (1), 11297. https://doi.org/10.1038/ncomms11297.

(7) Zhang, Z.; Xie, F.; Jia, J.; Zhang, W. Chiral Bicycle Imidazole Nucleophilic Catalysts: Rational Design, Facile Synthesis, and Successful Application in Asymmetric Steglich Rearrangement. *J. Am. Chem. Soc.* **2010**, *132* (45), 15939–15941. https://doi.org/10.1021/ja109069k.

(8) Nguyen, H. V.; Butler, D. C. D.; Richards, C. J. A Metallocene-Pyrrolidinopyridine Nucleophilic Catalyst for Asymmetric Synthesis. *Org. Lett.* **2006**, *8* (4), 769–772.

https://doi.org/10.1021/ol053050n.

(9) Shaw, S. A.; Aleman, P.; Christy, J.; Kampf, J. W.; Va, P.; Vedejs, E. Enantioselective TADMAP-Catalyzed Carboxyl Migration Reactions for the Synthesis of Stereogenic Quaternary Carbon. *J. Am. Chem. Soc.* **2006**, *128* (3), 925–934. https://doi.org/10.1021/ja056150x.

(10) De, C. K.; Mittal, N.; Seidel, D. A Dual-Catalysis Approach to the Asymmetric Steglich Rearrangement and Catalytic Enantioselective Addition of O-Acylated Azlactones to Isoquinolines. *J. Am. Chem. Soc.* **2011**, *133* (42), 16802–16805. https://doi.org/10.1021/ja208156z.

(11) Campbell, C. D.; Concellón, C.; Smith, A. D. Catalytic Enantioselective Steglich Rearrangements Using Chiral N-Heterocyclic Carbenes. *Tetrahedron: Asymmetry* **2011**, *22* (7), 797–811. https://doi.org/10.1016/j.tetasy.2011.04.001.

(12) de Castro, P. P.; Carpanez, A. G.; Amarante, G. W. Azlactone Reaction Developments. *Chem. Eur. J.* **2016**, *22* (30), 10294–10318. https://doi.org/10.1002/chem.201600071.

(13) Marra, I. F. S.; de Castro, P. P.; Amarante, G. W. Recent Advances in Azlactone Transformations. *Eur. J. Org. Chem.* **2019**, *2019* (34), 5830–5855. https://doi.org/10.1002/ejoc.201901076.

(14) Capreti, N. M. R.; Jurberg, I. D. Michael Addition of Soft Carbon Nucleophiles to Alkylidene Isoxazol-5-Ones: A Divergent Entry to β-Branched Carbonyl Compounds. *Org. Lett.* **2015**, *17* (10), 2490–2493. https://doi.org/10.1021/acs.orglett.5b01004.

(15) Jurberg, I. D. An Aminocatalyzed Stereoselective Strategy for the Formal α-Propargylation of Ketones. *Chem. Eur. J.* **2017**, *23* (41), 9716–9720. https://doi.org/10.1002/chem.201701433.

(16) Jurberg, I. D.; Davies, H. M. L. Rhodium- and Non-Metal-Catalyzed Approaches for the Conversion of Isoxazol-5-Ones to 2,3-Dihydro-6 H -1,3-Oxazin-6-Ones. *Org. Lett.* **2017**, *19* (19), 5158–5161. https://doi.org/10.1021/acs.orglett.7b02436.

(17) da Silva, A.; Fernandes, A.; Thurow, S.; Stivanin, M.; Jurberg, I. Isoxazol-5-Ones as Strategic Building Blocks in Organic Synthesis. *Synthesis (Stuttg).* **2018**, *50* (13), 2473–2489. https://doi.org/10.1055/s-0036-1589534.

(18) Ahn, S.; Hong, M.; Sundararajan, M.; Ess, D. H.; Baik, M.-H. Design and Optimization of Catalysts Based on Mechanistic Insights Derived from Quantum Chemical Reaction Modeling. *Chem. Rev.* **2019**, *119* (11), 6509–6560. https://doi.org/10.1021/acs.chemrev.9b00073.

(19) Freeze, J. G.; Kelly, H. R.; Batista, V. S. Search for Catalysts by Inverse Design: Artificial Intelligence, Mountain Climbers, and Alchemists. *Chem. Rev.* **2019**, *119* (11), 6595–6612. https://doi.org/10.1021/acs.chemrev.8b00759.

(20) Gould, E.; Walden, D. M.; Kasten, K.; Johnston, R. C.; Wu, J.; Slawin, A. M. Z.; Mustard, T. J. L.; Johnston, B.; Davies, T.; Ha-Yeon Cheong, P.; et al. Catalyst Selective and Regiodivergent O- to C- or N-Carboxyl Transfer of Pyrazolyl Carbonates: Synthetic and Computational Studies. *Chem. Sci.* **2014**, *5* (9), 3651. https://doi.org/10.1039/C4SC00879K.

(21) Marra, I. F. S.; de Almeida, A. M.; Silva, L. P.; de Castro, P. P.; Corrêa, C. C.; Amarante, G. W. Stereoselective Intermolecular [2 + 2] Cycloadditions of Erlenmeyer–Plöchl Azlactones Using Visible Light Photoredox Catalysis. *J. Org. Chem.* **2018**, *83* (24), 15144–15154. https://doi.org/10.1021/acs.joc.8b02430.

(22) Pinheiro, D. L. J.; Ávila, E. P.; Batista, G. M. F.; Amarante, G. W. Chemoselective Reduction of Azlactones Using Schwartz's Reagent. *J. Org. Chem.* **2017**, *82* (11), 5981–5985. https://doi.org/10.1021/acs.joc.7b00820.

(23) Frisch, M. J.; Trucks, G. W.; Schlegel, H. B.; Scuseria, G. E.; Robb, M. A.; Cheeseman, J. R.; Scalmani, G.; Barone, V.; Mennucci, B.; Petersson, G. A.; et al. Gaussian 09, Revision D.01. Gaussian, Inc.: Wallingford CT 2013.

(24) Grimme, S.; Antony, J.; Ehrlich, S.; Krieg, H. A Consistent and Accurate Ab Initio

Parametrization of Density Functional Dispersion Correction (DFT-D) for the 94 Elements H-Pu. *J. Chem. Phys.* **2010**, *132* (15), 154104. https://doi.org/10.1063/1.3382344.

(25) Zhao, Y.; Truhlar, D. G. The M06 Suite of Density Functionals for Main Group Thermochemistry, Thermochemical Kinetics, Noncovalent Interactions, Excited States, and Transition Elements: Two New Functionals and Systematic Testing of Four M06-Class Functionals and 12 Other Function. *Theor. Chem. Acc.* **2008**, *120* (1–3), 215–241. https://doi.org/10.1007/s00214-007-0310-x.

(26) Schlegel, H. B. Optimization of Equilibrium Geometries and Transition Structures. *J. Comput. Chem.* **1982**, *3* (2), 214–218. https://doi.org/10.1002/jcc.540030212.

(27) Maeda, S.; Harabuchi, Y.; Ono, Y.; Taketsugu, T.; Morokuma, K. Intrinsic Reaction Coordinate: Calculation, Bifurcation, and Automated Search. *Int. J. Quantum Chem.* **2015**, *115* (5), 258–269. https://doi.org/10.1002/qua.24757.

(28) Sinnokrot, M. O.; Valeev, E. F.; Sherrill, C. D. Estimates of the Ab Initio Limit for Π–π Interactions: The Benzene Dimer. *J. Am. Chem. Soc.* **2002**, *124* (36), 10887–10893. https://doi.org/10.1021/ja025896h.

(29) Too, P. C.; Wang, Y.-F.; Chiba, S. Rhodium(III)-Catalyzed Synthesis of Isoquinolines from Aryl Ketone O -Acyloxime Derivatives and Internal Alkynes. *Org. Lett.* **2010**, *12* (24), 5688–5691. https://doi.org/10.1021/ol102504b.

(30) Ablajan, K.; Xiamuxi, H. The Convenient Synthesis of 4-Arylmethylidene-4,5- Dihydro-3-Phenylisoxazol-5-Ones. *Chinese Chem. Lett.* **2011**, *22* (2), 151–154. https://doi.org/10.1016/j.cclet.2010.09.023.

(31) Fernandes, A. A. G.; Stivanin, M. L.; Jurberg, I. D. RuCl 3 / PPh 3 - Catalyzed Direct Conversion of Isoxazol-5-ones to 2,3-Disubstituted Pyridines. *ChemistrySelect* **2019**, *4* (12), 3360–3365. https://doi.org/10.1002/slct.201900761.

(32) Zhang, H.; Wang, B.; Cui, L.; Bao, X.; Qu, J.; Song, Y. Organocatalytic Asymmetric Fluorination of 4-Substituted Isoxazolinones. *Eur. J. Org. Chem.* **2015**, *2015* (10), 2143–

2147. https://doi.org/10.1002/ejoc.201500046.